Flight control of hybrid drones towards enabling parcel relay manoeuvres

Bruno Neves[1] and Bruno Guerreiro[1,2]
[1]DEEC and CTS/UNINOVA, NOVA School of Science and Technology, 2829-516 Caparica, Portugal.
[2]Institute For Systems and Robotics, LARSyS, 1049-001, Lisbon, Portugal.
E-mails: bms.neves@campus.fct.unl.pt and bj.guerreiro@fct.unl.pt

***Abstract*—This work addresses the modeling and controlling process of a hybrid unmanned aerial vehicle (UAV), aimed for parcel delivery with relay maneuvers. Hybrid UAVs bring significant advantages to the drone industry and related applications, such as the capability of flying in two flight modes, rotary and fixed-wing. Nonetheless, this versatility implies the added complexity both in modeling and controlling these vehicles. This work is based on a popular airframe, the Convergence tilt tri-rotor UAV, for which the overall system dynamics for all operation modes are deduced with plausible assumptions. The model is then validated by designing two separate controllers for the main flight modes, rotary and fixed-wing, capable of trajectory tracking in each mode. The control strategy makes use of a custom hybrid control allocation technique that differentiates the control in three parts: vertical, horizontal, and transitional flight modes. Finally, a hybrid controller is proposed, using a finite state machine capable of handling logical events, with the aim to provide control logic to perform autonomous mid flight transitions. The proposed control strategies are validated using Matlab.**

***Index Terms*—Hybrid UAV, UAV modeling, Transitional flight, Control Allocation, Hybrid Control**

I. Introduction

With the recent developments being made in all the areas surrounding unmanned aerial vehicles (UAV), or drones, such as sensors, computing power, and automotive industry, a UAV is becoming more resourceful and useful for many situations in the most diverse areas. The inspiration for this thesis comes from that fuss and development around UAVs to test and determine their capabilities in one of the most important industries, logistics, more precisely on parcel delivery techniques. Taking on that, this project was made to determine and test the capability and the possibility of creating a parcel delivering robust system, using one or multiple UAVs. UAVs can solve many problems and bring a lot of advantages to ease industries such as efficiency and automation. In short, the project seeks to understand and test all the possible advantages and disadvantages of bringing a hybrid UAV to the parcel delivering game. This creates new scientific challenges on trajectory planning, aggressive maneuvers, localization estimative, control techniques, hybrid control and so others. These indicated, that powerful systems need to be created in order to take the full advantages of using this technology in a new context.s.

* This work was partially funded by FCT project REPLACE (PTDC/EEI-AUT/32107/2017) which includes Lisboa 2020 and PIDDAC funds, project CAPTURE (PTDC/EEI-AUT/1732/2020), and also projects CTS (UIDB/00066/2020) and LARSYS (UIDB/50009/2020).

A. Motivation & Objective

In the scope of this project, we start with the knowledge gathered from previous works done on multi-rotors, being the most common a quadrotor. This work builds on the existing work and expands it to a solution of Hybrid drones also know as Vertical Take-Off and Landing (VTOL) vehicles. This type of UAV is getting more attention due to its advantages in endurance, efficiency, speed, manoeuvrability and modular approach over the more convectional drones [1]. For their use we need to devise strategies for modelling, design and control of hybrid drones to take full advantage of their capabilities.

A hybrid drone main difference is that they contain two flight modes, rotary-wing and fixed-wing. While the fixed-wing flight mode extends its maneuverability, the rotary-wing flight mode is used for more speed and propulsion efficiency being able to cover larger distances faster and using less energy when compared to a conventional multi-rotor drone, a workaround to the typical low flight times. This work will focus on creating a operational controller for a hybrid drone for further testing. The main objective is the implementation of a non-linear hybrid control system on a Hybrid UAV.

This work comes from the added complexity in the control of such type of UAV, unlike a quad-rotor, When less rotors are available, a mechanism normally controlled by a small servo motor is able to tilt two or three rotors independently, or in a joint motion(connected by a shaft), being this the reason tri-rotor UAVs are able to perform rotation in the three axis and are able to fly in different modes.

To make it perform, transition between states need to be addressed. Works like [2] and [3] show us the separation of flight modes, usually with two or three modes when added the transition mode. Despite this, the transitions between then don't seem to get the necessary attention or some possibilities are ignored. The main contributions of this paper are the development of model and integrated nonlinear controller for both rotary and fixed-wing modes of the Convergence hybrid drone, the a simple allocation method to obtaining the desired forces and moments from the available actuators for each of these modes, and the proposal of a hybrid controller for the overall system, which is validated through simulation.

The paper is organized as follows. Section II presents the model of the Convergence hybrid drone, Section III presents the nonlinear controllers for rotary and fixed-wing modes, while Section IV deals with the control allocation problem for the rotary and fixed-wing modes, but also for the transition mode. The overall hybrid controller is proposed in Section V and validated with simulation results in Section VI, while some concluding remarks and future work are offered in Section VII.

II. Modeling a Hybrid UAV

For simplifications purposes the model will be presented in two parts, forces and moments. In each one we will start by the effects of the rotors forces and then to the aerodynamics forces that enable the type of vehicle to perform as a fixed-wing. To develop the model some assumptions were made in order to make the process less complex, with minimal influence in most flight conditions.

- The UAV will be considered a rigid body with a fixed center of mass;
- Aerodynamic forces will only be generated by the rotor and wing;
- The fuselage drag forces are neglected;
- Wind will be neglected, so the groudspeed is equal to the airspeed on the body.

A. Vehicle characteristics

To know the capabilities of a hybrid tri-rotor with front tilt mechanism, we will take a look at all of the available actuators and control surfaces providing a simplified explanation of their main uses. The vehicle is composed of three rotors in a T configuration, they provide all the necessary thrust. Note that in rotary-wing flight the back rotor will be off. To make the mode transition possible, both front rotors have an independent servo motor that enables them to rotate in the y body axis. And finally the elevons act as control surfaces to be used in fixed wing mode to provide roll and pitch moments.

Throughout this work, some geometric constants will be brought upon, that are relative to the geometry of the drone, mainly the position coordinates of the three rotors and tilt angles and deflection angles. They are all present in Figure 1 where all the lengths are relative to the center of mass, represented by COM.

Two coordinate systems will be used: $W = \{W_x, W_y, W_z\}$ representing the stationary world frame in order with the ENU(East-North-UP) convention, with W_z being perpendicular to the ground plane and pointing upward; $B = \{B_x, B_y, B_z\}$ represents the body frame attached to the tilt-rotor centre of mass with B_x being the forward direction and B_z perpendicular to the drone plane in the upward direction. The rotation between the world frame and body frame depend on the Euler angles such that, roll ϕ, pitch θ and yaw ψ represent the rotation in x , y, z axis respectively, it will be donated by,${}^{W}R_{B}$, or by R for simplicity, a rotation matrix obtained from multiplying each rotation matrix Z-X-Y in this specific order.

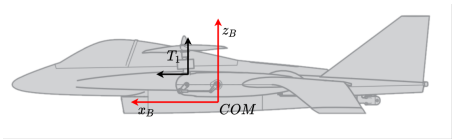

(a)

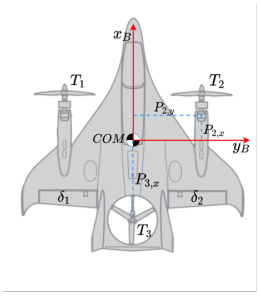

(b)

Fig. 1. Side view representing tilt mechanism (a) and top view (b) representing all actuators and Body axis

The angular velocity of the body frame relatively to the world frame is denoted by $\omega_B = [p, q, r]^T$, these values are the derivatives of roll ϕ, pitch θ and yaw ϕ such that

$$\omega_B = \begin{bmatrix} c_\theta & 0 & -c_\phi s_\theta \\ 0 & 1 & s_\theta \\ s_\theta & 0 & c_\phi c_\theta \end{bmatrix} \begin{bmatrix} \dot{\phi} \\ \dot{\theta} \\ \dot{\psi} \end{bmatrix}. \tag{1}$$

The tilt-rotor consists of three rotors capable of producing a lifting force in the positive B_z axis. Two of these rotors can be rotated independently in the B_y axis and the produced angle is given by α_1 for rotor 1 and α_2 for rotor 2. Each motor is able to produce a force, F_i, with its angular speed ω_i given by, $F_i = k_F \omega_i^2$. Being k_F a system constant relative to the used motor model. The resulting force exerted on the body is expressed by

$$F_i^B = \begin{bmatrix} F_i^{B_x} & F_i^{B_y} & F_i^{B_z} \end{bmatrix}^T \tag{2}$$

$$F_i^B = \begin{bmatrix} F_i s_{\alpha_i} & 0 & F_i c_{\alpha_i} \end{bmatrix}^T, \quad i = 1, 2 \tag{3}$$

$$F_3^B = \begin{bmatrix} 0 & 0 & F_3 \end{bmatrix}^T. \tag{4}$$

For the aerodynamics forces two main relevant forces are exerted on the body of the UAV: the drag force, D, and the lift force L. These forces are dependent on a series of characteristics of the drone's body shape, they can be simplified using a drag and lift coefficients, C_D, C_L. Both of these coefficients are dependent of the angle of attack(AoA), α. [4] For relatively small roll and pitch angles, where is planed the drone to be within, the values can be simplified into two curves dependent on the AoA [5].

$$C_L = C_{L_0} + C_{L_\alpha}\alpha\,, \quad C_D = C_{D_0} + C_{DC_L} C_L^2 \tag{5}$$

where, $C_{L_0}, C_{L_\alpha}, C_{D_0}$, are fixed values representing lift and drag at zero values and the respectively curve slope, C_{DC_L},

the induced drag derivative. From this, the simulated drag and lift forces can be calculated.

$$D = \bar{q}SC_D\,,\quad L = \bar{q}SC_L\,,\quad \bar{q} = \frac{1}{2}\rho V_a^2 \tag{6}$$

being ρ the air density and V_a the wind speed. This forces are applied to the COM like so,

$$F_a^B = \begin{bmatrix} c_\alpha & 0 & -s_\alpha \\ 0 & 0 & 0 \\ s_\alpha & 0 & c_\alpha \end{bmatrix} \begin{bmatrix} -D \\ 0 \\ L \end{bmatrix}. \tag{7}$$

Now we can obtain the net force expressed in the body frame,

$$F^B = \sum_{i=1}^{3} F_i^B + F_a^B \tag{8}$$

Each motor also produces two forms of moments exerted on the hub of each motor. The first one is due to the propeller drag, $M_{D,i}$, given by $M_{D,i} = k_M\omega_i^2$. The second form appears when a rotor is commanded to tilt, thus producing a small gyroscopic effect generating the moment $M_{G,i}$ given by $M_{G,i} = I_i(\dot{\Gamma}_i \times \omega_i)$, where I_i represents the propeller inertia and $\Gamma_i = [0\ \dot{\alpha}_i\ 0]^T$. These values now need to be expressed relatively to the tri-rotor body rotation. For that a rotation matrix,${}^BR_P$, converts from the rotor shaft rotation to the body frame like so

$${}^BR_P = \begin{bmatrix} c_{\alpha_i} & 0 & s_{\alpha_i} \\ 0 & 1 & 0 \\ -s_{\alpha_i} & 0 & c_{\alpha_i} \end{bmatrix}. \tag{9}$$

The tri-rotor design of the drone will also have a moment effect relative to the position of the three rotors, that is obtained with the cross product of the force vector and the vector between the centre of mass and the propeller. With $P_i = [P_{i,x}\ P_{i,y}\ P_{i,z}]$ being the rotor hub position relative to the body frame and h_P the distance between the hub and the rotor propeller. With this notation, we can present the position vector of each rotor propeller relative to the centre of mass, r_i, expressed in the body frame B

$$r_i = \begin{bmatrix} P_{i,x} + h_P s_{\alpha_i} & P_{i,y} & P_{i,z} + h_P c_{\alpha_i} \end{bmatrix}^T,\ i = 1, 2 \tag{10}$$

$$r_3 = \begin{bmatrix} P_{3,x} & P_{3,y} & P_{3,z} \end{bmatrix}^T \tag{11}$$

For the aerodynamics induced moments we have the roll and pitch moments produced by the elevons.

$$M_a^B = \bar{q}SL_e \begin{bmatrix} C_r & C_p & 0 \end{bmatrix}^T \tag{12}$$

where $L_e = diag(E_y, E_x, E_z)$, is the position relatively to the center of mass of the elevons and $C_r,\ C_p$ the roll and pitch aerodynamic coefficients dependent on the elevon deflection angle.

The total torque matrix applied to the the center of mass is a sum of the aerodynamic torques and rotor torques expressed as

$$M^B = \sum_{i=1}^{3} {}^BR_P(M_{D,i} + M_{G,i}) + \sum_{i=1}^{3}(F_i^B \times r_i) + M_a^B. \tag{13}$$

B. System Dynamics

Knowing the forces exerted on the drone's body, by Newton's equations of motions, its possible to obtain the system dynamics containing the linear acceleration $\dot{\nu}$ and angular acceleration $\dot{\omega}_B$ in the following equation:

$$\begin{aligned} \dot{p} &= \nu \\ \dot{\nu} &= -gW_z + \frac{1}{m}RF^B \\ \dot{\omega}_B &= I^{-1}(-\hat{\omega}_B I\omega_B + M^B) \\ \dot{R} &= R\hat{\omega}_B. \end{aligned} \tag{14}$$

Where g is the gravitational acceleration, m is the body mass, I the moment of inertia, and $\hat{\omega}_B$ is the skew matrix resulting from ω_B. The vehicle position is $p = [p_x, p_y, p_z]^T$ and the velocity $v = [v_x, v_y, v_z]^T$ of the body frame described in the world frame. These equations describe the system state, with them it is possible to obtain the updated body states in each step from the controller inputs.

III. Control Design

In this section, lays the implementation of the autopilot controller proposed in order to command the UAV in both flight modes. The objective of such controller is to, knowing the state x,

$$x = [p^T, v^T, \omega_B^T, vec(R)^T] \tag{15}$$

of the vehicle, where the operator $vec(.)$ denotes the vectorization of the argument matrix and the desired trajectory, output the desired thrust and torque components, $u = [F, M^B] = [u_x, u_y, u_z, \tau_x, \tau_y, \tau_z]^T$, where $F = RF^B$, that will enable the UAV to follow the desired flight path.

Because of the major difference between control methods in the two main flight modes of the UAV, two separate control algorithms with the same base approach yet with different outcomes were developed. One of them will focus on rotary-wing flight mode as for the second, it will just be used when the vehicle is in fixed-wing flight mode. This solution discards, for now, the problem that will appear when the UAV is in a transition mode, later, on this work we will see that this problem can be overcome with a semi-hybrid control output involving both of these controllers.

The proposed controller implementation will be based on the work [6], [7], it contains a trajectory tracking controller designed specifically for a quad-rotor UAV. The bases of the controller still apply for a tri-rotor UAV. With some alterations and different tuning it can be perfected for our case. As for the fixed wing controller, a separate controller with further design modification will be proposed in order to account for the special system dynamics in such flight mode.

A. Rotary-wing control law

In the Rotary-wing flight mode controller, the base design of the work [6] is kept almost intact. We calculate position and velocity errors based on a predefined reference trajectory.

Adding a proportional gain, K_p, K_v, as positive gain matrices the desired force vector is calculated as

$$F_{des} = -K_p e_p - K_v e_v + mgz_W + ma_{ref} \tag{16}$$

with $e_p = p - p_{ref}$ and $e_v = v - v_{ref}$. The first input u_1(thrust command), can be computed as a projection of the desired force vector into the body frame z_B coincident with the drone thrust vector

$$u_z = F_{des} \cdot z_B. \tag{17}$$

After this the procedure is to calculate the desired rotation matrix as,

$$R_{des} = [x_{B_{des}}, y_{B_{des}}, z_{B_{des}}]^T, \tag{18}$$

And from there the desired angular velocity, w_{Bdes}. With both of this values the rotation error, e_R and the angular velocity error, e_w can be calculated and multiplied by the last two gain matrices, K_r and K_w, rotational and angular gains respectively. Giving us finally the last thre outputs,

$$M^B_{des} = [\tau_x, \tau_y, \tau_z]^T = -K_r e_R - K_\omega e_\omega. \tag{19}$$

with $e_\omega = \omega_B - \omega_{Bdes}$ and $e_R = \frac{1}{2}(R^T_{des}R - R^T R_{des})^\vee$, being $\vee$ the vee map operand(skew matrix inverse).

B. Fixed-wing control

For the Fixed-wing flight mode, the controller needs to be redesigned to cope with the physical changes in the system. The main changes concerning the design of the controller are:

- Only the two front rotors are active and rotated 90°, producing now a forward thrust force in the direction of the body axis x_B;
- Resulting from the increased speed, aerodynamic forces such as lift and drag, now need to be accounted for;
- The yaw angle, ψ is now constrained with the direction of the trajectory of flight and no longer given as a reference. This is due to the flight dynamics of a fixed wing, where yaw is directly correlated to the direction of movement minus minor drifts.

The first step remains the same, calculating the position errors, but now these are calculated in respective to the auxiliary frame A. The auxiliary frame corresponds to the world frame, W, with and added rotation in the z_W axis, so that x_A axis direction is always in the same direction as the current body yaw angle. We define a Rotation matrix that transforms between the world frame and the auxiliary frame,

$${}^W R_A = \begin{bmatrix} \cos\psi & \sin\psi & 0 \\ -\sin\psi & \cos\psi & 0 \\ 0 & 0 & 1 \end{bmatrix}. \tag{20}$$

Now the desired force F^A_{des} will be relative to the auxiliary frame A. As we have two more main forces acting on the body, drag and lift, the desired force F^A_{des} will have to account for them. The desired force is now computed as

$$F^A_{des} = {}^W R^T_A[-K_p e_p - K_v e_v + mgz_W + ma_{ref}] - {}^A R_B(L+D) \tag{21}$$

With this, the thrust command can be obtained being, the projection of the desired force onto x_B axis, where the thrust force is directed, $u_x = F^A_{des} \cdot x_B$.

For the attitude loop, the objective is once more obtain the desired rotation, R_{des}. But now a different method needs to be developed in order to cope with the physical changes in the system. Firstly, as a fixed wing generates the majority of the net force in the x_B axis, corresponding to the direction of thrust, meaning, its movement direction in normal conditions is close to the x_B direction(with a low angle of attack)(In other words, the aircraft moves roughly to where the nose points). We assume $x_{B_{des}}$ as the direction of F^A_{des},

$$x_{B_{des}} = \frac{F^A_{des}}{\left\| F^A_{des} \right\|}. \tag{22}$$

As we know, a fixed wing aircraft achieves a change of direction in the xy plane with a roll moment, a rotation in the x_B axis. The roll rotation will be commanded by the direction of $y_{B_{des}}$ so

$$y_{B_{des}} = \frac{[0, x_{By}, x_{Bx}]^T \times x_A}{\| [0, x_{By}, x_{Bx}]^T \times x_A \|} \tag{23}$$

with $x_A = [1, 0, 0]^T$ and $x_{B_{des}} = [x_{Bx}, x_{By}, x_{Bz}]^T$. Then $z_{B_{des}}$ becomes

$$z_{B_des} = x_{B_{des}} \times y_{B_{des}}. \tag{24}$$

Finally, the only step left is bringing the calculated rotation to the world frame again by rotating it over the z_W axis.The required rotation is equal to the desired yaw angle, ψ_{des} defined as

$$\psi_{des} = \begin{cases} -\arccos \frac{v_x}{\sqrt{v_x^2 + v_y^2}} & v_y \leq 0 \\ \arccos \frac{v_x}{\sqrt{v_x^2 + v_y^2}} & v_y > 0 \end{cases} \tag{25}$$

Note the yaw angle is relative to the X_W axis belonging to the interval $-180° < \psi_{des} \leq 180°$. Becoming

$${}^W R_{Bdes} = \begin{bmatrix} c_{\psi_{des}} & -s_{\psi_{des}} & 0 \\ s_{\psi_{des}} & c_{\psi_{des}} & 0 \\ 0 & 0 & 1 \end{bmatrix} [x_{B_{des}}, y_{B_{des}}, z_{B_{des}}]. \tag{26}$$

From this point on, until the last three input commands, the same tri-rotor control laws apply, equation (21).

It is important to note that this design assumes a reference trajectory that is inline with a fixed-wing aircraft capabilities, and a more exotic trajectory may not have the desired performance. This leaves space for further development of an optimal trajectory generation, that is left for future work.

IV. Control Allocation

To obtain a full fledged control system one must obtain the desired actuator control signal. To do so a final step, named control allocation, will transform the output of the controller designed in Section III, namely the force and moments values, to real actuator settings, mapping them so that the UAV will produce the desired force and torque. This process is known as control allocation.

The objective is to find the effectiveness matrix, G, that solves the following equation

$$u_W = G^{-1}u \tag{27}$$

being u_w, the actuator vector containing all actuator settings. In this case it contains 7 values, 3 rotor speeds ,w_i, two tilt angles α_i and 2 elevons angles δ_e and δ_a

$$u_w = \begin{bmatrix} w_1^2 & w_2^2 & w_3^2 & \alpha_1 & \alpha_2 & \delta_e & \delta_a \end{bmatrix}^T. \tag{28}$$

After the control allocation, in a STIL (Software-In-the-Loop) simulation, the end result is then mapped to PWM values and sent to the UAV controller unit. However, in the mathematical simulation, the actuator values are then mapped again to forces and torques via the equations presented in Section II and sent to the system dynamics loop.

A. Effectiveness Matrices

In the following sections, three different effectiveness matrices will be obtained for different flight modes: tri-rotor, fixed-wing and transition. Each one will use different actuators, being this a over actuated system, with 4DOF(Degrees Of freedom) to seven actuator inputs, although some of the actuators inputs are coupled. This gact enables the use of various control approaches, note that the ones shown on this work were tested and found to be fit to the problem showing great overall performance.

1) Rotary-wing: For this VTOL state, both elevons will be ignored since they provide low to none influence at the low speed this flight mode is aimed for. Using only the three rotors will generate an under actuated system, so five inputs will be used: 3 rotors speeds and the tilt angles of the two front rotors. The following equations represent the output forces and torques connection to the input actuator settings

$$\begin{cases} F_z = k_F w_1^2 c_{\alpha_1} + k_F w_2^2 c_{\alpha_2} + k_F w_3 \\ \tau_x = r_{1y} k_F w_1^2 c_{\alpha_1} + k_M w_1^2 s_{\alpha_1} + r_{2y} k_F w_2^2 c_{\alpha_2} - k_M w_2^2 s_{\alpha_2} \\ \tau_y = r_{1x} k_F w_1^2 c_{\alpha_1} + r_{2x} k_F w_2^2 c_{\alpha_2} + r_{3x} k_F w_2^2 \\ \tau_z = r_{1y} k_F w_1^2 s_{\alpha_1} + k_M w_1^2 c_{\alpha_1} + r_{2y} k_F w_2^2 s_{\alpha_2} - k_M w_1^2 c_{\alpha_2} + k_M w_3^2 \end{cases} \tag{29}$$

where $r_{ix/y}$ represents the rotor distance to the center of mass in x and y axis. Looking into the equation system, it's obvious that it is nonlinear and if arranging the system to accommodate the template in equation (27), the effectiveness matrix G would not be invertible. To overcome this problem, the system of equation was linearized trough first order Taylor's series expansion around a equilibrium point. The linearization process can be tedious and quite a stretch to enumerate so the end result, will not be presented here, for further reference see [8].

For this setup, the equilibrium point used is relative to the actuator settings providing a stable hover flight. Away from hover, the equilibrium point is updated every time step to the last output implying that the effectiveness matrix changes dynamically every time step. Although this method could result in jittering for changing the allocation matrix so fast, the results were found to be very good. In case it is necessary this process can be changed to only update the equilibrium point when the linearization error overcomes a constant value, saving computational power. To obtain the desired actuator settings one must then, invert the effectiveness matrix G, in this specific case using the Moore–Penrose. inverse

2) Fixed Wing: The proposed allocation technique for the rotary-wing flight mode fixes three controller inputs namely, both tilt servo motors and the back rotor. They will not be used in this mode, this makes the control allocation behave like a conventional aircraft equipped with elevons. Now the velocities achieved are high enough to create lift and produce both roll and pitch moments with only the elevon action. Both rotors are tilted $90°$ producing a constant force in the positive body axis, x_B direction. They are also able to produce yaw moment and consequently a unwanted minimal roll moment created by the propeller drag that is counteracted by the elevons. Using equation (13) and (8) it's possible to arrive to the 4DOF equations and then arrive to the effectiveness matrix G,

$$G = \begin{bmatrix} k_F & k_F & 0 & 0 \\ k_M & -k_M & \bar{q}SE_y C_{r\delta} & 0 \\ 0 & 0 & 0 & \bar{q}SE_x C_{p\delta} \\ r_{1_y} k_F & -r_{2_y} k_F & 0 & 0 \end{bmatrix} \tag{30}$$

Note that $\bar{q}$ contains a system variable, airspeed, meaning that the effectiveness's matrix will dynamical change over time. As it is a square matrix it can be easily inverted so the actuator settings are then obtained by solving the following equation.

$$\begin{bmatrix} w_1^2 \\ w_2^2 \\ \delta_a \\ \delta_e \end{bmatrix} = G^{-1} \begin{bmatrix} F_x \\ \tau_x \\ \tau_y - \bar{q}SE_x(C_{p_0} + C_{p_\alpha}\alpha) \\ \tau_y \end{bmatrix} \tag{31}$$

3) Transition: In this phase the main objective is to bring the tilt rotor angle to a fixed position, $90°$ for a fixed-wing to rotary-wing flight transition and $0°$ for a rotary-wing to fixed-wing flight transition in the shortest time possible. When a transition is commanded, both tilt servo motors will have a fixed desired angle, meaning that they will not serve as control actuators on this phase. Therefore, the remaining five actuators, $w_1, w_2, w_3\delta_a$, and δ_e will be responsible for the 4DOF system. Another point to consider is the thrust input. On previous flight modes thrust was orientated in the z_B or x_B direction, as the rotor tilt angle will now constantly change, the direction of thrust follows the same direction. So for this allocation we assume the thrust input is already oriented in the actual direction of the tilt angle, $\bar{\alpha} = \frac{\alpha_1 + \alpha_2}{2}$. The thrust force vector will be designated by $\vec{F_{zx}}$ so that, $\left\| \vec{F_{zx}} \right\| = u_t$, $\theta_F = \bar{\alpha}$. With this, the effectiveness matrix can be deduced by combining both the tri-rotor and fixed wing torque equations ending up with:

$$G = \begin{bmatrix} k_F & k_F & k_F c_{\bar{\alpha}} & 0 & 0 \\ r_{1y}k_F c_{\alpha_1} + k_M s_{\alpha_1} & r_{1y}k_F c_{\alpha_2} - k_M s_{\alpha_2} & 0 & \bar{q}SE_y C_{r\delta} & 0 \\ r_{1x}k_F c_{\alpha_1} & r_{2x}k_F c_{\alpha_2} & r_{3x}k_F & 0 & \bar{q}SE_x C_{p\delta} \\ r_{1y}k_F s_{\alpha_1} - k_M c_{\alpha_1} & r_{2y}k_F s_{\alpha_2} + k_M s_{\alpha_2} & k_M & 0 & 0 \end{bmatrix} \tag{32}$$

Applying the same process, inverting G, the actuator settings are calculated by solving equation (33).

$$\begin{bmatrix} w_1^2 & w_2^2 & w_3^2 & \delta_a & \delta_e \end{bmatrix}^T = G^+ \begin{bmatrix} \left\| \vec{F_{zx}} \right\| & \tau_x & \tau_y & \tau_y \end{bmatrix}^T \tag{33}$$

With this, all three matrices are defined. In the next Section, they will be used in conjunction to the hybrid controller, to simulate the drone's transitions on the mathematical model.

V. Hybrid Autopilot Controller

The goal of this controller is to achieve seamless transition without human interference or by hard-coded trajectory waypoints. The transition between flight modes is the controller decision, taken based on both trajectory reference and system state. To achieve this one must develop a hybrid system capable of transition between controllers developed in Section III.

In our case, three different control schemes (rotary-wing, fixed-wing, and transitional) will be joined in a single controller. To overtake this issue we use a finite state machine, FSM, to handle all discrete values and logical operations. The transition method is based on velocity, the idea is that depending on both the reference velocity and the actual velocity, the controller is able to adopt the most suitable flight mode for the case and if needed, perform a transition. To

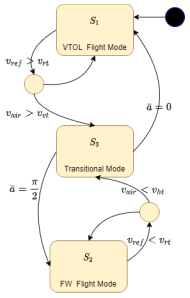

Fig. 2. Proposed control method block diagram

command transitions a mixing between the reference velocity magnitude and the actual airspeed will act as control variables for the FSM. The last variable is the determinant factor on defining flight modes, the rotor tilt angle, as we assume that a $90°$ angle corresponds to the rotary-wing flight mode and an approximate angle of $0°$ for the fixed-wing flight mode. In sum, the input control variables used for the design of the FSM are:

- $\|\mathbf{v_{ref}}\|$: Reference velocity magnitude.
- $\mathbf{v_{air}}$: The actual airspeed.
- $\bar{\mathbf{a}}$: Rotor tilt angle.

With these control variables, an algorithm was designed to commute between the three possible states, S_1, S_2, S_3, representing each flight mode, fixed-wing, rotary-wing and transitional respectively.

The event table presented in Table I shows all of the possible transitions of the FSM, using the three inputs available. The states represented in it are the possible transitions as also shown in Figure 2. With v_{vt}, v_{ht}, v_{rt}, fixed-wing, rotary-wing

TABLE I
Event based FSM table

State-Transition table			
Input \ Current state	$\mathbf{S_1}$	$\mathbf{S_2}$	$\mathbf{S_3}$
$\|v_{ref}\| > v_{rt} \wedge v_{air} > v_{vt}$	S_3		
$\|v_{ref}\| < v_{rt} \wedge v_{air} < v_{ht}$		S_3	
$\bar{a} = \frac{\pi}{2}$			S_2
$\bar{a} = 0$			S_1

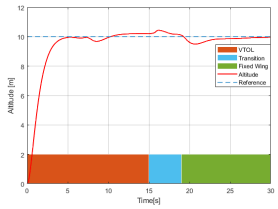

(a) Altitude

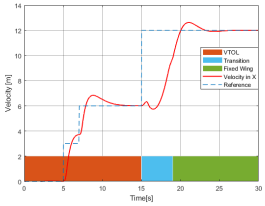

(b) Velocity

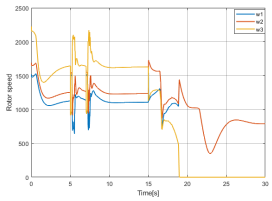

(c) desired rotors angular speed

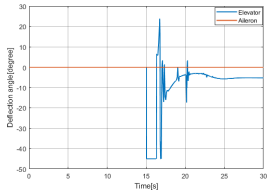

(d) desired elevator/aileron deflection

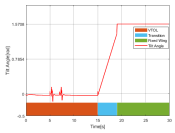

(e) tilt angle $\bar{a}$

Fig. 3. Positive transition simulation

and reference velocities respectively, that can be adjusted to the designer needs.

VI. Simulation

In order to simulate the system, it was modulated in Matlab/Simulink with a closed-loop configuration. Both model and system dynamics equations were reproduced in Matlab and populated with the Convergence tilt-rotor body specifications and custom gain matrices.

The first simulation procedure will test the performance of the hybrid controller on a positive transition, from fixed-wing to rotary-wing flight mode. The UAV will start at the origin, climb to a stable hover point and then gradually raises its velocity. Set-points will be used for the reference trajectory and then, we observe the UAV behavior when transitioning from VTOL to fixed wing flight. Note that the only human operator input is the pre-defined reference trajectory the hybrid controller handle everything else.

Figure 3 shows us, as expected at $t = 15\ s$ where the reference velocity exceeds the threshold value v_{rt}, the UVA

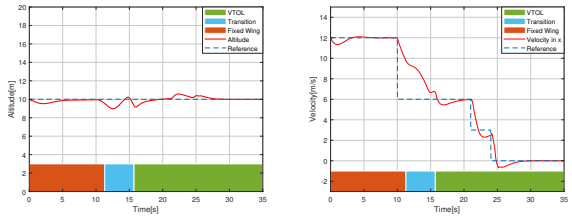

(a) Altitude

(b) Velocity

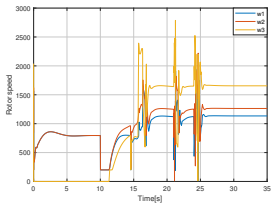

(c) desired rotors angular speed

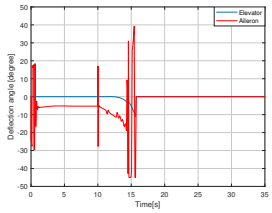

(d) desired elevator/aileron deflection

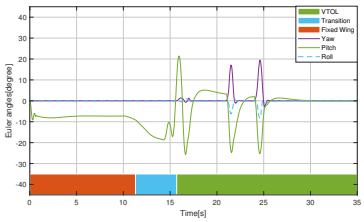

(e) Euler angles

Fig. 4. Negative transition simulation

begins a transition to the rotary-wing flight mode. Around $t = 19\ s$ the transition is completed, meaning that the rotor tilt angle $\bar{a}$ is fixed at $90°$, which is confirmed in Figure 3e. From there, the UAV is flying steady in the rotary-wing flight mode achieving the desired velocity of $12m/s$. In this transition, the altitude error was kept between $0.5 < e_{p_z} < 0.5\ m$, achieving a maximum value of $0.47\ m$, a relative low value when compared to the actual altitude this mode is designed to operate. Figure 3e show us the average tilt, $\frac{\alpha_1+\alpha_2}{2}$, angle quickly rises to the forward position when the UAV start the transition. The remaining actuator settings are showed in Figure 3c.

Proceeding with the simulation process, next a negative transition was simulated with the UAV, starting in the rotary-wing flight mode at a reference constant velocity. At $t = 10\ seconds$ a negative step in the reference velocity occurs, bringing the reference value lower than the threshold value, $v_h t$. The UAV then is forced to reduce its speed and perform a transition to fixed-wing flight mode because of the major lift fore reduction due to the velocity decrees.

This time, the transition although expected, induced a higher altitude drop, figure 4, achieving a minimum value of $1\ m$ below the reference altitude. This shows a struggle on the controller side when transiting to rotary-wing mode caused by two factors: the changing tilt angle and the lift force oscillation, due to the velocity decrease (also the AoA changes rapidly). The thrust component will struggle due to high side drift, causing a higher altitude drop that is still relatively low.

As for the UAV velocity, we can notice here a slower deceleration curve, being the wind resistance the only force acting on it in fixed wing mode. And again, near the transition end, $t = 15.7\ s$, the oscillations become more noticeable. This can happen due to a side effect of the pitch angle readjusting. In rotary-wing flight, mode the pitch tends to be a few degrees over the xy world frame plane in order to raise the angle of attack. On the other hand in fixed-wing flight mode the pitch is below the reference level so the rotors generate force in the x_W axis enabling the UAV to maintain its velocity. In this scenario the change occurs at a speed that the lift forces are still high enough to be noticeable, with the changing angle of attack the UAV becomes more unstable. A good solution for this would be to have dynamic rotation gains in the hybrid controller so that the UAV had lower torque forces near transitions than in normal conditions.

VII. Conclusion

A model of a generalized tilt-rotor hybrid UAV was developed in order to test a hybrid control technique with the goal of achieving automated and smooth flight smooth transition. With the implementation of a control allocation technique designed for each flight mode, the system was mathematically simulated in a closed-loop. The hybrid controller showed cable of performing transitions when necessary, being the only input a predefined reference trajectory. Both transitions occurred smoothly with no oscillations and with a minimal drop in altitude.

For future work, the controller is left ready to be implemented in a real scenario using the Convergence tilt rotor. Preferably using the PX4 framework alongside Pixhawk hardware. Also the controller can be further tested in a realistic environment using ROS+GAZEBO with the autopilot software in the loop (SITL).

References

[1] A. S. Saeed, A. B. Younes, C. Cai, and G. Cai, "A survey of hybrid unmanned aerial vehicles," *Progress in Aerospace Sciences*, vol. 98, pp. 91–105, 2018.

[2] X. Fang, Q. Lin, Y. Wang, and L. Zheng, "Control strategy design for the transitional mode of tiltrotor uav," in *IEEE 10th International Conference on Industrial Informatics*. IEEE, 2012, pp. 248–253.

[3] G. R. Flores-Colunga and R. Lozano-Leal, "A nonlinear control law for hover to level flight for the quad tilt-rotor uav," *IFAC Proceedings Volumes*, vol. 47, no. 3, pp. 11 055–11 059, 2014.

[4] B. L. Stevens, F. L. Lewis, and E. N. Johnson, *Aircraft control and simulation: dynamics, controls design, and autonomous systems*. John Wiley & Sons, 2015.

[5] W. Rigon Silva, A. da Silva, and H. Gründling, "Modelling, simulation and control of a fixed-wing unmanned aerial vehicle (uav)," 12 2017.

[6] D. W. Mellinger, "Trajectory generation and control for quadrotors," 2012.

[7] M. Marques, B. J. Guerreiro, R. Cunha, and C. Silvestre, "Trajectory planning and control for drone replacement for multidrone cinematography," *IFAC-PapersOnLine*, vol. 52, no. 12, pp. 334–339, 2019.

[8] B. M. Neves, "Flight control of hybrid drones towards enabling parcel relay manoeuvres," Master's thesis, NOVA University of Lisbon, 2021. [Online]. Available: http://users.isr.ist.utl.pt/ bguerreiro/students/2021_BNeves_MSc_Thesis.pdf